We think, however, that the proposed mechanism is a good first approximation.

Key experimental aspects of hydrogenation employed in deriving our proposed version of the Horiuti–Polanyi mechanism on platinum are old: the nearly irreversible adsorptions of olefin[11] and of hydrogen.[21] A possible role of gaps in the surface layer in permitting some interconversion of para- and orthohydrogen was proposed long ago.[21] Further, our model has features in common with some other mechanistic proposals. For the hydrogenation of cyclohexene in the vicinity of room temperature, Madon, O'Connell, and Boudart[22] concluded that "the measured rate is that of chemisorption of dihydrogen on a metal surface covered with reactive hydrocarbon intermediate". Although we disagree with their assumption that olefin adsorption is in preequilibrium, for a reaction of zero order in olefin, reversible adsorption will lead to the same kinetic form for the rate (but not for formation of isomerized olefin). Reference 22 also assumes that hydrogen adsorption occurs at gaps in the layer of adsorbed olefin, but it assumes that the adsorption occurs on a carbonaceous layer which almost completely covers the metal. We believe that recent work in this laboratory[23] establishes that at ambient temperatures the hydrogenation reaction occurs directly on the platinum surface. There is also agreement that hydrogen spillover contributes negligibly to the reaction. In particular, we have shown[24] that covering the silica surface of Pt/SiO_2 by $OSi(CH_3)_3$ had a negligible effect upon the rate of hydrogenation of cyclopentene.

In a recent study of the reaction between deuterium and propylene on evaporated rhodium,[25] the rates of desorption of hydrogen and of olefin were both shown to be slow. The authors concluded that "hydrogen adsorption under the retardation of adsorbed propene rate-determines propene hydrogenation over Rh". Despite the nonstandard use of *rate-determining process*,[26] the ideas are close to those expressed in the present paper. The authors[25] consider that the fact that the rate of hydrogenation of ethylene is about twice that of propylene to be "related to adsorption heat of olefin and the number of surface sites occupied by one molecule of adsorbed olefin", whereas we consider the heat of adsorption to be irrelevant once it is strong enough to give zero-order kinetics, and we think it is the gaps in the packing that are determining rather than the number of sites occupied by one molecule of olefin.

Structure Sensitivity. Why should the effect of varying particle size on overall rates of hydrogenation be so small?[12,22] On our model, one must assume that the effective area of the gaps would vary little between various crystal planes and edges. This seems to be a plausible assumption, and it corresponds to that in ref 22 about the effective area of the gaps in a carbonaceous overlayer on these planes and edges. However, structure sensitivity could still be substantial in the selectivities observed in competitive runs, particularly those involving hindered olefins,[12] since selectivity depends upon competition in the adsorption step (like eq 4).

Acknowledgment. Acknowledgment is made to the donors of the Petroleum Research Fund, administered by the American Chemical Society, for the support of this research. We are indebted to Dr. R. Pitchai for measuring the percentage exposed of platinum on 0.2-Pt-952. R.L.B., Jr. is also indebted to the Humboldt Stiftung for a Senior Scientist Award during the tenure of which at the Technical University Munich this paper was written.

Registry No. TMPNO, 2564-83-2; TMP, 768-66-1; Pt, 7440-06-4; SiO_2, 7631-86-9; cyclopentene, 142-29-0.

---

[21] Eley, D. D. In "Catalysis", Emmett, P. H., Ed.; Reinhold: New York, 1955; Vol. 3, p 63.

[22] Madon, R. J.; O'Connell, J. P.; Boudart, M. *AIChE J.* **1978**, *24*, 904–911.

[23] Hattori, T.; Burwell, R. L., Jr. *J. Phys. Chem.* **1979**, *83*, 241–249.

[24] Kung, H. H.; Brookes, B. I.; Burwell, R. L., Jr. *J. Phys. Chem.* **1974**, *78*, 875–878.

[25] Sato, S.; Iyama, T.; Miyahara, K. *J. Catal.* **1981**, *69*, 77–88.

[26] Boudart, M. "Kinetics of Chemical Processes"; Prentice-Hall: Englewood Cliffs, NJ, 1968.

A Theoretical Study of the Acetaldehyde-Derived Radical

Earl S. Huyser,[†] David Feller, Weston T. Borden, and Ernest R. Davidson*

Contribution from the Department of Chemistry, University of Washington, Seattle, Washington 98195. *Received November 4, 1981*

Abstract: Relative stabilities and selected properties for the two lowest lying doublet states of the acetaldehyde-derived radical have been determined with large basis set MCSCF/CI wave functions. The energy gap is seen to be quite sensitive to the choice of basis set and CI orbital space.

The stability of carbon-centered free radicals α to a carbonyl function is generally ascribed to delocalization of the unpaired electron between the carbon atom and the oxygen of the carbonyl function.[1]

This stability is reflected, in part, by the reactivities of α,β-unsaturated carbonyl-containing compounds toward addition by free radicals and hydrogen atom abstraction from the α-carbon of carbonyl-containing compounds. Since the resonance structures of this radical

are reminiscent of those of enolate anions, species which display ambident anionic character (e.g., capable of both C-alkylation and O-alkylation in nucleophilic displacement reactions),[2] ambident character might be expected for α-carbonyl radicals as well. However, there is no experimental evidence for such behavior,

---

[1] Walling, C. "Free Radicals in Solution", Wiley: New York, 1957; p 51.

[2] See: Carey, F. A.; Sundberg, R. J. "Advanced Organic Chemistry"; Plenum Press: New York, 1977; pp 15–19.

nor would it be readily expected. The propensity for oxygen-centered radicals to add to alkene linkages is considerably less than that of carbon-centered radicals. This has led to the prediction, consistent with observation, that α-carbonyl radical additions involve carbon–carbon bond formation. Although hydrogen atom abstraction by oxygen-centered radicals is generally more favorable than by carbon-centered radicals, the vinyl alcohol formed would tautomerize to the reaction product predicted if the abstraction involved initial formation of the carbon–hydrogen bond. Thus, while experimental detection of ambident character in hydrogen atom abstraction reactions by α-carbonyl radicals through product identification is precluded, the possibility of such behavior exists.

The α-carbonyl radical system also presents a further interesting possibility in that the pertinent nuclear centers possess C_s symmetry so that the radical may exist in two different electronic states, namely, the $^2A'$ and the $^2A''$ states. Recent work suggests that the chemical behavior of such a radical may be dependent on its electronic state.[3] It is also possible that the ambident character of the α-carbonyl radical may be greater in one state than in the other.

Optical absorption studies using the technique of photochemical modulation spectroscopy have recently been completed by Hunziker, Kneppe, and Wendt[4] on the primary radical products of oxygen atom–olefin reactions. They found CH_2CHO to be an important primary product of reactions with ethylene or monosubstituted ethylenes. Earlier experimental work on this radical by Cvetanovic[5] employed mass-spectrometric sampling techniques to analyze the final reaction products of atomic oxygen. Lee et al.[6] and Luntz and Kleinermans[7] have studied mechanisms for the formation of CH_2CHO with molecular beam techniques. Inoue and Akimoto[8] have reported laser-induced fluorescence from an excited state at 3.57 eV.

From a theoretical perspective, current interest in the vinoxy radical centers on the energy gap separating the $^2A''$ ground state and the low-lying $^2A'$ state. For obvious reasons, we shall sometimes refer to the former as the "π" radical and the latter as the "σ". The only previously published theoretical work on this radical is that of Baird and Taylor,[9] who performed minimal basis set configuration interaction (CI) calculations. Because of the uncertainties introduced by the use of a small basis and limited geometry optimization, they regarded their calculated gap of 5.9 kcal/mol as "very tentative". During the course of this investigation, we have also learned of multiconfiguration SCF (MCSCF) calculations on the X^2A', $1^2A''$, and $^2A'$ states of CH_2CHO by Dupuis, Wendoloski, and Lester.[10]

Procedure

Any theoretical investigation of the σ–π energy difference must start with the recognition that, although this radical is ostensibly capable of being described by a single electronic configuration, restricted Hartree–Fock (RHF) calculations on the $^2A''$ state will be plagued by the so-called "doublet instability" problem. While this effect has been extensively studied for such cases as the allyl radical, CH_2CHCH_2,[11] in heteroatom molecules, such as CH_2CHO, its presence is less obvious.

For π radicals this instability is characterized by the tendency of RHF wave functions to localize the odd electron and thus lead to broken symmetry solutions of the RHF equations even at symmetric geometries. While localization of the odd electron and π bond is indeed the correct behavior for sufficiently long bond lengths, the persistence of such a structure at near-equilibrium bond lengths as the lowest energy form of the radical has been shown to be an artifact of RHF wave functions. The magnitude of the effect is largest for minimal basis sets but persists even with near HF limit basis sets.

Table I. Optimal Geometry Parameters and Total Energies (in Hartrees)

state	basis	type	R-(C–C)^a	R-(C–O)	∠CCO	energy
$^2A''$	STO-3G	RHF	1.486	1.224	123.3	−150.3039
		RHF	1.316	1.408	122.0	−150.3189
		UHF	1.406	1.341	122.1	−150.3468
		MCSCF	1.403	1.326	122.2	−150.3726
	3-21G	RHF	1.450	1.217	123.7	−151.4285
		RHF	1.316	1.384	120.8	−151.4292
		UHF	1.382	1.301	122.3	−151.4515
		MCSCF	1.409	1.272	122.4	−151.4759
	SV	SDQ-CI^b				−152.541
	SVP	SDQ-CI^b				−152.749
		RHF^c	1.464	1.198	123.9	−152.3234
		RHF^c	1.335	1.325	120.8	−152.3044
		MCSCF^d	1.442	1.227	122.5	−152.3554
		SDQ-CI^e				−152.467
		SDQ-CI^f				−152.762
	experimental		1.48	1.27		
$^2A'$	STO-3G	RHF	1.311	1.404	123.7	−150.3228
		UHF	1.345	1.407	123.3	−150.3266
		MCSCF	1.343	1.404	123.2	−150.3639
	3-21G	RHF	1.311	1.385	123.1	−151.4254
		UHF	1.312	1.383	125.3	−151.4272
		MCSCF	1.331	1.390	124.5	−151.4546
	SV	SDQ-CI^b				−152.518
	SVP	SDQ-CI^b				−152.728
		RHF^c	1.323	1.342	125.0	−152.3002
		MCSCF^d	1.340	1.347	124.4	−152.3211
		SDQ-CI^c				−152.428
		SDQ-CI^f				−152.735

^{a} Bond lengths are given in angstroms. Bond angles are shown in degrees. ^{b} This wave function was computed at the optimal 3-21G MCSCF geometry. ^{c} Dupuis et al.[10] ^{d} This basis contained one set of d primitives on the two carbons and oxygen. No p primitives were added to the hydrogen basis functions. ^{e} Excitations allowed within the conceptual minimal basis set space only. ^{f} Performed at the preceding optimal geometry.

As anticipated, RHF calculations with the STO-3G[12] basis yielded two distinct $^2A''$ minima, corresponding to the two resonance structures, $H_2C—CH=O$ and $H_2C=CH—O$. Unless otherwise noted, all geometry optimizations were performed with GAMESS,[13] an analytical gradient RHF/GVB/MCSCF program from the National Resource for Computation in Chemistry. Structures were considered to be converged when the largest component of the gradient was less than 0.001 hartree/bohr. STO-3G RHF values of the C–C and C–O bond lengths and the CCO bond angle are given in Table I along with the experimental geometry of Inoue and Akimoto. The C=C minimum is 9.4 kcal/mol below the corresponding C=O minimum.

The doublet instability phenomenon may be viewed as an inadequacy of RHF wave functions which results from the inability to describe adequately the electrostatic repulsion of the two opposite spin π electrons, in this case one from the bonding orbital and the odd electron in the nonbonding orbital. The RHF wave function is forced to localize the odd electron and π bond at opposite ends of the allyl radical in order to minimize this repulsion. In contrast to this, spin-polarized unrestricted Hartree–Fock (UHF), by permitting a buildup of negative spin density

---

(3) For example, see: Skell, P. S.; May, D. D. *J. Am. Chem. Soc.*, **1981**, 103, 967. Skell, P. S.; Day, J. C. *Acc. Chem. Res.*, **1978**, *11*, 381. Koenig, T.; Wielesek, R. A.; Huntingdon, J. G. *Tetrahedron Lett.*, **1974**, *26*, 2283. Kikuchi, O. *ibid.*, **1977**, *28*, 2421. McBride, J. M.; Merrill, R. A. *J. Am. Chem. Soc.*, **1980**, *102*, 1723.

(4) Hunziker, H. E.; Kneppe, H.; Wendt, H. R., private communication.

(5) Cvetanovic, R. J. *Adv. Photochem.*, **1963**, *1*, 115.

(6) Lee, Y. T., lecture presented at the 14th Informal Conference on Photochemistry, Newport Beach, CA, April 1980.

(7) Luntz, A.; Kleinermans, K. *J. Phys. Chem.*, to be published.

(8) Inoue, G.; Akimoto, H. *J. Chem. Phys.*, **1981**, *74*, 425.

(9) Baird, N. C.; Taylor, K. F. *Can. J. Chem.*, **1980**, *58*, 733.

(10) Dupuis, M.; Wendoloski, J. J.; Lester, W. A., Jr. *J. Chem. Phys.*, to be published.

(11) Paldus, J.; Veillard, A. *Mol. Phys.*, **1978**, *35*, 445.

(12) Hehre, W. J.; Stewart, R. F.; Pople, J. A. *J. Chem. Phys.*, **1969**, *51*, 2657.

(13) Dupuis, M.; Spangler, D.; Wendoloski, J. J. NRCC Software Catalog, Prog. No. QG01, GAMESS, 1980, Vol. 1.

(14) Elbert, S. T.; Cheung, L. M.; Ruedenberg, K. NRCC Software Catalog, Prog. No. QM01, ALIS, 1980, Vol. 1.

Table II. $^2A'' - {}^2A'$ Energy Gap

basis	wave function	geometry	ΔE, kcal/mol
STO-3G	UHF	optimal UHF	12.7
	MCSCF	optimal MCSCF	5.5
3-21G	UHF	optimal UHF	15.2
	MCSCF	optimal MCSCF	13.5
SV	SDQ-CI (estd)	optimal 3-21G MCSCF	14.4
SVP	SDQ-CI (estd)	optimal 3-21G MCSCF	13.6
	MCSCF	optimal RHF[a]	19.7
	MCSCF	optimal MCSCF	21.5
	SDQ-CI[b]	optimal MCSCF	24.4
	SDQ-CI	optimal MCSCF	16.9
	exptl[c]		22.8

[a] Reference 10. [b] Excitations within the conceptual minimal basis set space only. [c] Reference 4.

on the central carbon (assuming the odd electron is spin up), does not suffer from the problem. The optimal STO-3G UHF bond lengths, shown in Table I, are approximately the average of the two corresponding RHF values. A spin population analysis of the UHF wave function shows essentially three unpaired electrons.

Small basis set UHF calculations, benefiting from a fortuitous cancellation of errors, may sometimes yield relative energies that are qualitatively superior to more elaborate computational methods. However, in general they cannot be expected to yield quantitatively reliable energies if there exists any differential correlation effects. Interestingly, the STO-3G UHF value of 12.7 is more than twice the MCSCF value. Therefore, we performed full MCSCF calculations in the orbital space of one σ and three π orbitals. Although full π space MCSCF would have been sufficient to avoid the doublet instability problem, the addition of the σ orbital was judged to give a more evenhanded description of the two states. Its inclusion resulted in the addition of three more configurations to the $^2A''$ list, for a total of 11 spin-adapted configurations. The optimal $^2A''$ geometry parameters, shown in Table I, are quite close to the UHF values. Also shown in the table are the optimal $^2A'$ geometries obtained from analogous calculations on the higher energy state. The configuration list for this state consisted of nine spin-adapted configurations.

The σ–π gaps, computed with the STO-3G UHF and MCSCF wave functions, are listed in Table II. The gap obtained by Dupuis et al. with a smaller configuration space is 4.6 kcal/mol, in close agreement with our value of 5.5 kcal/mol. Interestingly, the STO-3G UHF value of 12.7 is more than twice the MCSCF value. However, neither is in very good agreement with the experimental estimate.

As seen in Table II, enlargement of the basis set to the 3-21G[15] level substantially improves the MCSCF estimate of the energy gap while only moderately improving the UHF value. The 3-21G full π space MCSCF value of Dupuis et al. is again quite close, at 12.5 kcal/mol. Table I shows that in contrast to the STO-3G case, the 3-21G basis, presumably by alleviating some of the well-known deficiencies of the minimal basis in describing π electrons, yields two RHF $^2A''$ minima which are essentially degenerate. While the UHF and MCSCF geometries are still averages of the two minima, they are no longer in quite as good agreement with each other as they were with the minimal basis. The computed gap is still only 59% of the experimental value.

In order to determine if recovery of a larger fraction of the valence correlation energy would improve agreement with experiment for the σ–π gap, we performed CI calculations involving all single and double excitations from the HF configuration. For enhancement of the convergence properties of the CI, the unoccupied orbitals were transformed to K orbitals.[16] Tests on a growing number of molecules indicates that this transformation results in a substantial improvement in CI convergence. A K-orbital CI with the same configuration list as was used in the MCSCF calculations produced an energy within 5 mhartree of the MCSCF energy. This amounted to about 85% of the energy lowering obtained with MCSCF orbitals. For the $^2A''$ state, the K-orbital CI recovered 81% of the estimated total valence correlation energy while an SCF-CI of the same length recovered only 63%. Second-order perturbation theory was used to select the 500 most important space orbital products (1665 spin-adapted configurations) from among the full set of 6432 space products. The quantity of energy ignored by excluding the remainder of the configurations was estimated by scaling the perturbation theory estimate of this quantity by the ratio of the actual CI energy lowering (with respect to the HF energy) divided by the perturbation theory estimate of the CI lowering. When 80% or more of the correlation energy is variationally recovered, this estimate is usually accurate to several percent, a few millihartrees in this case. A correction was likewise made for the effects of neglected quadruple excitations.[17] The SDQ-CI energies with the Dunning[18] [3s,2p/2s] split valence (SV) contraction of Huzinaga's[19] (9s,5p/4s) basis are listed in Table I. As seen in Table II, the computed σ–π gap is still only 14.4 kcal/mol.

One set of d-type polarization functions (carbon exponent = 0.75, oxygen exponent = 0.85) and one set of p type (hydrogen exponent = 1.2) were added to the basis set to obtain a split valence plus polarization (SVP) basis. When SDQ-CI calculations were performed with this enlarged basis at the optimal 3-21G MCSCF geometries, a σ–π gap of 13.6 kcal/mol (which represents a small decrease) was obtained. Some 2200 space orbital products (7800 spin-adapted configurations) were retained from the total of 29 000 single and double excitation space products. This list contained all 531 single excitations. Approximately 80% of the total estimated correlation energy was variationally recovered.

If the optimal $^2A''$ MCSCF geometry is viewed as an energy-weighted average of the RHF minima, there is reason to suspect that further improvement in the energy gap could be obtained by optimizing the π radical geometry with d functions in the basis set. Previous RHF calculations have shown that one set of d functions will lower the energy of a C–O double bond by about twice as much as it will a C–C double bond. Indeed, Baird and Taylor have suggested the importance of d functions for π radicals, but because of the computational expense have failed to add such functions to their basis sets. On the basis of RHF geometry optimizations with d functions, Dupuis et al. have also suggested that these functions are crucial to accurately describe the π state. Their SVP MCSCF calculations at the optimal RHF geometries gave a σ–π gap of 19.8 kcal/mol.

We have extended the calculations of Dupuis et al. by actually performing d function MCSCF geometry optimization of the two states. No p functions were added to the hydrogen basis sets, since these were judged to be relatively unimportant for accurately describing the main geometric differences between the two radicals in the C–C and C–O bond lengths. Portions of the early SVP MCSCF geometry optimizations were performed with the program ALIS.[14] Final structures were obtained with GAMESS. The final MCSCF geometries are shown in Figure 1 and, for comparison's sake, are also listed in Table I. Agreement to several hundredths of an angstrom with the SVP RHF geometries was obtained. Our MCSCF energy gap of 21.5 kcal/mol is slightly closer to the experimental value than the 19.8 kcal/mol of Dupuis et al.

K-orbital SD-CI calculations were performed at the optimal SVP MCSCF geometries. Excitations were limited to the conceptual minimal basis space, i.e., the orbital space generated by considering only the occupied atomic symmetries— (1s, 2s, 2p) for carbon and oxygen, (1s) for hydrogen. All 4825 $^2A''$ (5570 $^2A'$) spin-adapted configurations were included. The SVP basis, with p functions on the hydrogens, was used. The energy gap obtained was 23.5 kcal/mol, or 24.4 kcal/mol if the quadruples correction was made.

---

(15) Binkley, J. S.; Pople, J. A.; Hehre, W. J. *J. Am. Chem. Soc.*, **1980**, *102*, 939.

(16) Feller, D.; Davidson, E. R. *J. Chem. Phys.*, **1981**, *74*, 3977.

(17) Davidson, E. R. In "The World of Quantum Chemistry", Daudel, R., Pullman, B., Eds.; Reidel: Dordrecht, Netherlands, 1974.

(18) Dunning, T. H., Jr.; Hay, P. J. In "Modern Theoretical Chemistry", Schaefer, H. F., III., Ed.; Plenum Press: New York, 1977; Vol. 2.

(19) Huzinaga, S. *J. Chem. Phys.* **1965**, *42*, 1293.

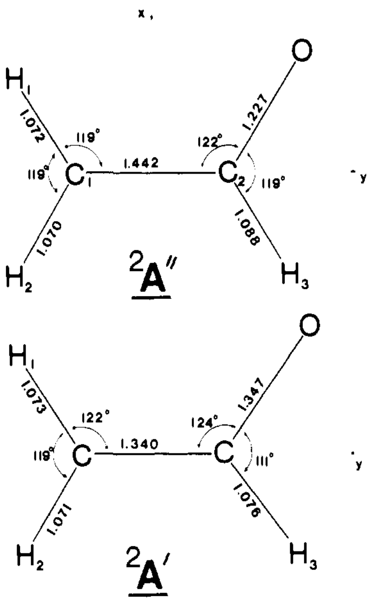

Figure 1. Optimal geometry from an MCSCF calculation with the split valence–polarization basis set.

Numerous chemists, both experimentalists and theoreticians, employ the notion of a conceptual minimal basis set space. Ruedenberg and co-workers,[20] for example, have demonstrated the utility of this space in computing molecular MCSCF reaction energies. With the proviso that those orbitals that are unoccupied in the HF configuration are redefined by some suitable procedure (MCSCF, K orbitals, Iterative Natural Orbitals, etc.), the SDQ-CI result within this space should yield reasonable results.

An analysis of the CI wave functions for the two states reveals a very similar list of configurations in the top ten, ordered with respect to energy contributions. In both states the HF configuration entered the CI wavefunction with an expansion coefficient of 0.968, followed by a double excitation (a single in the σ space coupled with a single in the π space) with an expansion coefficient of 0.1. The remaining eight configurations are also easily matched between the two CI vectors.

When the orbital space was expanded to include the entire basis set, perturbation theory was again required to reduce the number of configurations to the size indicated above (about 7800 spin-adapted configurations). The computed gap was 17.5 kcal/mol (16.9 kcal/mol with quadruples correction). While it is possible that the procedure we employed to account for the neglected double excitations could be in error, the size of the disagreement between the conceptual minimal basis set CI and the full basis set CI seems to indicate a real difference of at least several kcal/mol.

Values of selected properties obtained with the SVP SD-CI wave functions are given in Table III. The molecule lies in the xy plane with the CC bond extending along the x axis, as is indicated in Figure 1.

Table III. Selected SVP Basis SD-CI Properties

property	$^2A''$ results	$^2A'$ results
x dipole, D	−2.319	−1.303
y dipole, D	−2.192	−0.278
dipole moment, D	3.191	1.332
field gradient[a] at C_1, au	0.266	0.045
at C_2, au	0.461	0.131
O, au	1.442	2.313
del (spin)[b] at H_1, au	−0.011	−0.000
at H_2, au	−0.011	0.001
at H_3, au	−0.001	0.021
π spin pop at C_1	0.842	−0.005
at C_2	−0.025	−0.002
at O	0.166	0.009

[a] $(3z^2 - r^2)/r^5$ component. [b] Fermi contact term, $\delta(r_N)$, averaged with the spin density.

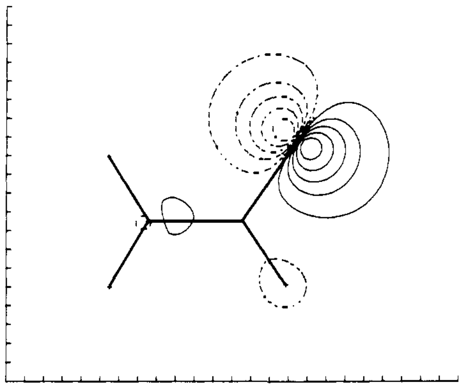

Figure 2. The singly occupied orbital in the $^2A'$ state. This is primarily an oxygen nonbonding p orbital.

While the rather larger dipole moment of the $^2A''$ state is approximately aligned with the C–O bond (negative end toward oxygen), the much smaller moment of the $^2A'$ state is oriented in the negative x direction. This difference results from the charge transfer associated with the migration of the unpaired electron or, alternatively, the "hole", from the terminal carbon in the former state to the oxygen in the latter. This migration is reflected in the π spin population data shown in Table III. A contour plot of the $^2A'$ singly occupied orbital density, displayed in Figure 2, shows the orbital to be a highly localized p orbital on oxygen.

The electric field gradient is a measure of the deviation from spherical symmetry at the nucleus. While the smaller positive value of the field gradient at oxygen in the $^2A''$ state shows some partial charge transfer commensurate with π-bond formation, the large negative value seen for the $^2A'$ state clearly reflects the loss of the in-plane electron at that atom.

Proton isotropic coupling constants were computed for the three hydrogen protons in the $^2A''$ state. The CI values at H1 and H2 are −0.011 au (−49.2 MHz), which is in qualitative agreement with the value predicted by McConnell's relationship, −57 MHz.

Acknowledgment. This work was supported in part by a grant from the National Science Foundation.

Registry No. Ethenyloxy, 6912-06-7; 2-oxyethyl, 4400-01-5.

---

(20) Ruedenberg, K.; Schmidt, M. W.; Dombek, M. G., private communication.

(21) McConnell, H. M.; Strathdee, J. *Mol. Phys.*, **1959**, *2*, 129.